International Journal of Mass Spectrometry 276 (2008) 91–101

Contents lists available at ScienceDirect

International Journal of Mass Spectrometry

journal homepage: www.elsevier.com/locate/ijms

Through-space and through-bond electron transfer within positively charged peptides in the gas phase

Diane Neff, Monika Sobczyk, Jack Simons*

Chemistry Department and Henry Eyring Center for Theoretical Chemistry, University of Utah, Salt Lake City, UT 84112, United States

ARTICLE INFO

Article history:
Received 30 January 2008
Received in revised form 15 April 2008
Accepted 21 April 2008
Available online 1 May 2008

Keywords:
Disulfide cleavage
Coulomb stabilization
Electron-capture dissociation
Electron-transfer dissociation
Electron transfer

ABSTRACT

Processes by which an electron, initially attached to a protonated or fixed-charge side chain, can (i) undergo through-bond transfer to migrate to an S—S σ* orbital and cleave a disulfide linkage, or (ii) undergo through-space transfer from that charged site to another positively charged side chain are examined using ab initio electronic structure methods. Earlier work from this group along these lines is extended in two directions:

1. The spacer units along which through-bond electron transfer occurs are extended to include olefinic as well as aliphatic units (because polypeptide backbones and side chains contain π as well as σ bonds).
2. The electron binding energies of positively charged side chains can vary substantially. In earlier work, protonated amine —NH_3^+ and fixed-charge —$N(CH_3)_3^+$ units were used as model systems. In this work, two positive units with more similar electron binding strengths are employed to see whether more facile electron transfer occurs when two such groups collide.

The primary findings are

1. That through-bond electron transfer through combined olefinic–aliphatic linkages is not qualitatively different (in rate) than through aliphatic linkages.
2. That through-bond transfer can occur to S—S bonds at experimentally relevant rates but only over ca. 7 intervening bonds.
3. That through-space transfer from one positive side chain to another can occur but only if the electron binding strengths of the two side chains' positive sites are similar.

1. Introduction and background

Electron-capture dissociation [1] (ECD) and electron-transfer dissociation [2] (ETD) mass spectroscopic methods have shown much utility and promise for sequencing peptides and proteins. A strongpoint of both techniques is their propensity for selectively cleaving disulfide and N—C_α bonds and for doing so over a wide range of the backbone, thus producing many different fragment ions. Parallel with many advances in the experimental development and improvement of these methods, theoretical studies have been carried out to try to determine the mechanism(s) [3] by which electron attachment leads to these bond cleavages.

In our earlier efforts [3h–3m,3o,3p] to explore how ETD or ECD electrons can cleave S—S or N—C_α bonds in positively charged gas-phase peptides (e.g., as exist under electrospray conditions in mass spectroscopy experiments), we proposed that electrons can attach directly (i.e., in a nearly vertical exothermic process) to S—S σ* or OCN amide π* orbitals, but only under special conditions. In particular, we suggested that such low-lying empty orbitals can have their energies lowered by attractive Coulomb interactions with one or more positively charged groups (e.g., the protonated amine or fixed-charge groups on side chains that usually exist in ECD/ETD experiments) thus rendering the electron attachment exothermic. In Scheme 1, we illustrate the mechanisms by which such electron attachment events are proposed to lead to cleavage of disulfide or N—C_α bonds through what we termed Coulomb-stabilized direct electron attachment.

We know from others' work on dissociative electron attachment [4] that, in the absence of Coulomb stabilization, vertical electron

* Corresponding author. Tel.: +1 801 581 8023.
E-mail address: simons@chem.utah.edu (J. Simons).
URL: http://simons.hec.utah.edu (J. Simons).

1387-3806/$ – see front matter © 2008 Elsevier B.V. All rights reserved.
doi:10.1016/j.ijms.2008.04.012

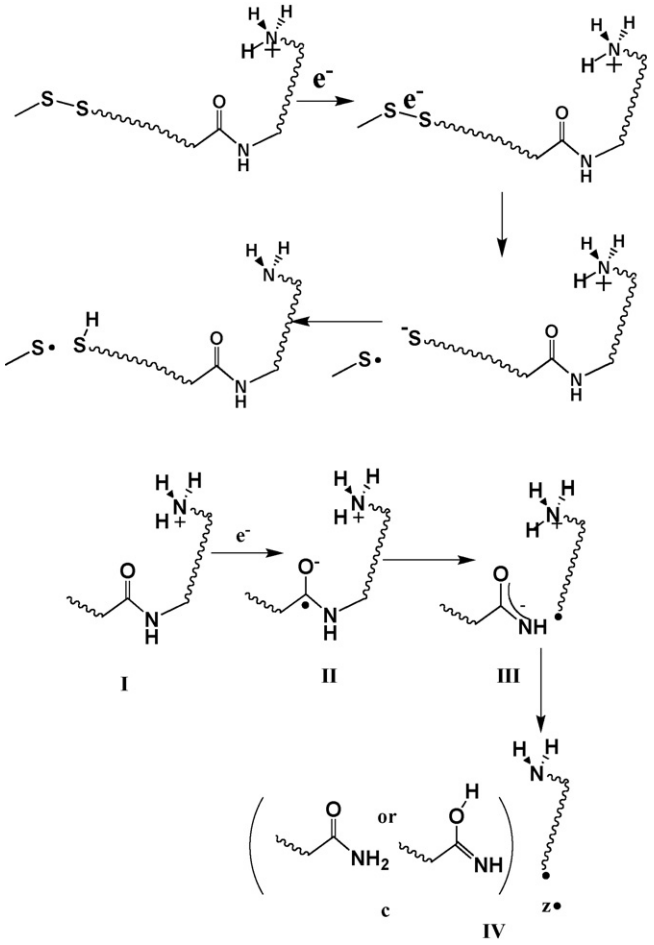

Scheme 1. Direct electron attachment to a Coulomb stabilized S—S σ* or OCN π* orbital to cleave a disulfide or N—C_α bond.

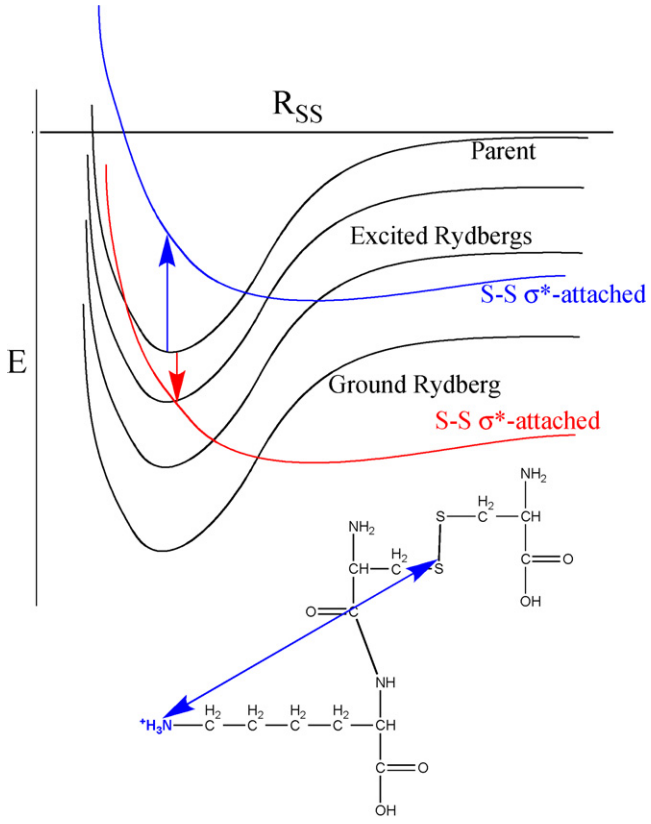

Fig. 1. Model disulfide containing peptide (bottom) with protonated Lys side chain together with energy profiles (top) along the S—S bond length for the parent compound, ground- and excited-Rydberg states with an electron attached to the Lys —NH_3^+ site, and the state in which the excess electron resides in the S—S σ* orbital.

attachment to an S—S σ* or amide π* orbital is ca. 1 eV and ca. 2.5 eV endothermic, respectively. Using the fact that the Coulomb potential varies with distance R (Å) as 14.4 eV Å/R (Å), we predicted under what structural circumstances such direct electron attachment should be expected. For example, we proposed that a disulfide linkage must experience Coulomb stabilization exceeding 1 eV to render our direct-attachment mechanism feasible; this stabilization could, for example, arise from a single positively charged site closer than ca. 14 Å, from two positive sites each 7 Å distant, or from a doubly charged site 28 Å away. We also predicted that a single positive charge 14.4/2.5 = 6 Å from an OCN π* orbital could render this orbital amenable to exothermic direct electron attachment.

To further explain our ideas about how the Coulomb-stabilized direct electron attachment takes place, in Fig. 1 we show qualitative depictions of the potential energy hypersurfaces of model species containing an S—S bond that is subject to such cleavage.

In our proposed mechanism, an electron (either a free electron as in ECD or one transferred from an anion as in ETD) can attach exothermically (red arrow in Fig. 1) to the S—S σ* orbital if the positively charged site on the Lys side chain is within 14 Å of the SS bond (red curve in Fig. 1). Once an electron attaches to the σ* orbital, rupture of the S—S bond occurs promptly. On the other hand, if the positive site is more than 14 Å away from the SS bond, electron attachment would be endothermic (blue arrow and blue curve) and thus would not occur under ECD/ETD conditions. Of course, in a multiply positively charged polypeptide, it is the total Coulomb stabilizing potential at the SS bond site that will determine the placement of the S—S σ* curve relative to that of the parent and Rydberg-attached species. Moreover, the magnitude of this Coulomb potential will depend on the location, along the backbone, of the positive sites and can fluctuate significantly as the charged side chains undergo dynamical motions.

In summary, our proposal was that the S—S σ* curve will lie vertically (i.e., near the equilibrium bond length of the S—S bond) below the parent if the total Coulomb stabilization at the S—S bond site exceeds ca. 1 eV, and, under such conditions, direct exothermic electron attachment to the S—S bond can occur. We and the Turecek group made an analogous suggestion for cleaving N—C_α bonds via direct Coulomb-stabilized electron attachment to OCN π* orbitals as suggested in Scheme 1. The energy profiles along the N—C_α bond axis for a model parent, Rydberg-attached, and OCN π*-attached species are shown in Fig. 2.

A significant difference between the S—S and N—C_α cleavage cases is that, in the latter, the electron attaches vertically to the OCN π* orbital to form the carbon-centered radical species shown in Fig. 2, but bond cleavage does not occur promptly as it does in the disulfide cleavage case. Instead, elongation of the N—C_α bond must occur (e.g., through thermal motions) to induce a crossing of this OCN π*-attached state with a state in which the excess electron resides in the N—C_α σ* orbital. Evolution of the electron density into this latter state allows the N—C_α bond to break upon which a new C—N π bond is formed and the radical center moves to the α-carbon site as shown in Fig. 2 and Scheme 1. Thus, although both disulfide and N—C_α cleavages are proposed to be initiated by Coulomb-assisted electron attachment, bond cleavage is prompt in the former case but requires surmounting a barrier (where the OCN π* and N—C_α σ* curves cross) in the latter.

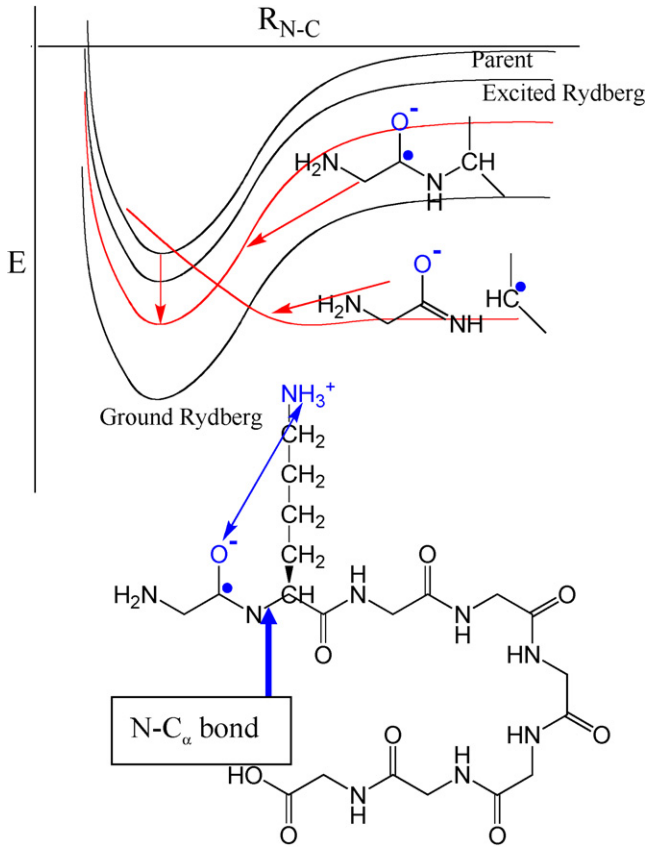

Fig. 2. Model peptide (bottom) with protonated Lys side chain together with energy profiles (top) along the N—C_α bond length for the parent compound, ground- and excited-Rydberg states with an electron attached to the Lys —NH_3^+ site, and the state in which the excess electron resides in the N—C_α π^* orbital (as shown in the model compound).

2. Overview of our earlier studies

The Coulomb-stabilized direct attachment model was used in Ref. [3j] to rationalize the distribution of fragment ions observed [5] under ECD conditions for the doubly charged peptide shown in Fig. 3.

Specifically, regardless of whether the number (n) of alanine units is 10, 15, or 20 and whether the parent ion is doubly protonated or doubly sodiated (presumably at the Lys sites), the main fragment ions arise from

a. S—S bond cleavage at the central site, or
b. N—C_α cleavage along the Ala backbone but only within the four Ala units closest to the positively charged Lys termini.

We noted that, even for $n = 20$, where the positively charged sites reside ca. 30 Å from the S—S bond, the Coulomb stabilization at the disulfide linkage (2×14.4 eV Å/30 Å) is ca. 1 eV-just enough to render exothermic Coulomb-stabilized attachment to the S—S bond. We also noted that the four Ala units nearest the termini lie ca. 6 Å from the positive sites, so their Coulomb stabilization energy[1] (1×14.4 eV Å/6 Å) is ca. 2.5 eV—again, just enough to stabilize the OCN π^* orbital to electron attachment.

Of course, the agreement between our model's predictions for the species shown in Fig. 3 may be fortuitous. Experiments in which the number of Ala units exceeds 20 (so the Coulomb stabilization at the S—S bond drops below 1 eV) or in which ETD rather than ECD is used (so electron attachment at the S—S site might be rendered endothermic for $n = 20$ because of the need to overcome the electron binding energy of the anion used as the electron source) would be welcome contributions to such studies.

In other studies exploring the Coulomb-stabilization model, we needed to address the possibility that electron attachment (ETD or ECD) could occur initially at a positively charged site (e.g., at one of the Lys termini of the species shown in Fig. 3) after which an electron could migrate to an S—S or OCN bond site to effect cleavage. This migration might occur in a through-space manner if the positively charged site's Rydberg orbital occupied by the excess electron were to come into spatial overlap with an S—S σ^* or an OCN π^* orbital. Alternatively, the migration could occur in a through-bond manner in which the positive site's Rydberg orbital overlaps with orbitals on intervening functional groups which subsequently overlap with an S—S σ^* or an OCN π^* orbital.

For the species shown in Fig. 3, the terminal Lys groups are so far from the S—S bond that through-space transfer to the S—S bond is not feasible. So, for this species, we focused on through-bond electron transfer by computing energy profiles analogous to those shown qualitatively in Fig. 1 for model compounds of the form H_3C—S—S—$(CH_2)_n$—NH_3^+. In these studies [3o,3q,3r], we held fixed the distance between the nitrogen atom and the S—S bond to simulate a fixed total Coulomb stabilization potential whose strength depended on the numbed n of methylene units. We then evaluated the energies, as functions of the S—S bond length, of states in which an excess electron is attached to a Rydberg orbital of the —NH_3^+ or to the Coulomb-stabilized S—S σ^* orbital. An example of our data is shown in Fig. 4 for the $n = 3$ case.

We also show in Fig. 4 the S—S σ^* (left), excited Rydberg (center), and ground Rydberg (right) orbitals so one can appreciate the spatial extent of these orbitals. In Fig. 5 we show these same sets of orbitals for the $n = 3$, 2, and 1 species again to allow the reader to appreciate how their spatial extent can produce significant couplings and thus allow electron migration to occur.

By examining the potential energy curves in regions where the S—S σ^* curve crosses either the ground or excited Rydberg curve, we were able to extract the electronic coupling strengths (denoted $H_{1,2}$) connecting these pairs of states. In Fig. 4, we give the values of these coupling strengths for the $n = 3$ species. As expected, we found the magnitudes of these electronic couplings to decay exponentially with the distance R between the S—S σ^* and Rydberg orbitals between which the through-bond migration takes place. In Fig. 6, we show how these couplings vary with distance [3q]. In this plot, the error bars relate to our estimated uncertainties in evaluating the $H_{1,2}$ values, and the points shown as open circles and squares are extrapolations of our data for $n = 1, 2, 3$, to the $n = 4$ case.

Using these data and Landau-Zener surface-hopping theory we were able to estimate that through-bond electron migration occur at rates that could lead to S—S bond cleavage within times appropriate to ECD/ETD conditions, but only over 4 or 5 bonds separating the nitrogen and sulfur atoms.[2] Thus, we are able to conclude that the S—S bond cleavage observed for the species shown in Fig. 3 did not arise from electron attachment at a positive Lys site followed by through-bond electron transfer to the S—S bond; the number of intervening bonds is far too large. At this stage in our studies, we

[1] In making this estimate, we ignore the Coulomb stabilization from the more distant Lys terminus, so the total Coulomb stabilization is a bit larger than this estimate.

[2] As we will show later, the combination of our earlier data and that obtained in the present work suggest that this estimate should probably be increased to 7 bonds.

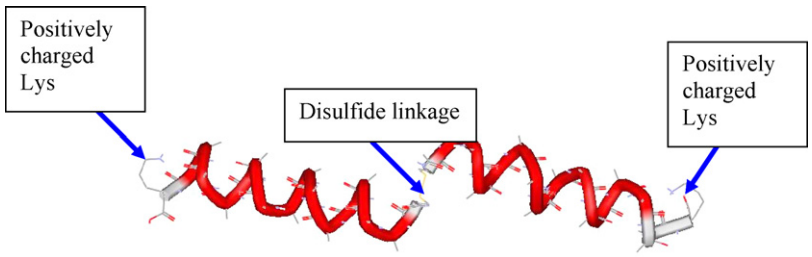

Fig. 3. Assumed structure of doubly charged $(AcCA_nK+M)_2^{2+}$ cations (M = H or Na) in gas phase (redrawn from Ref. [3j]).

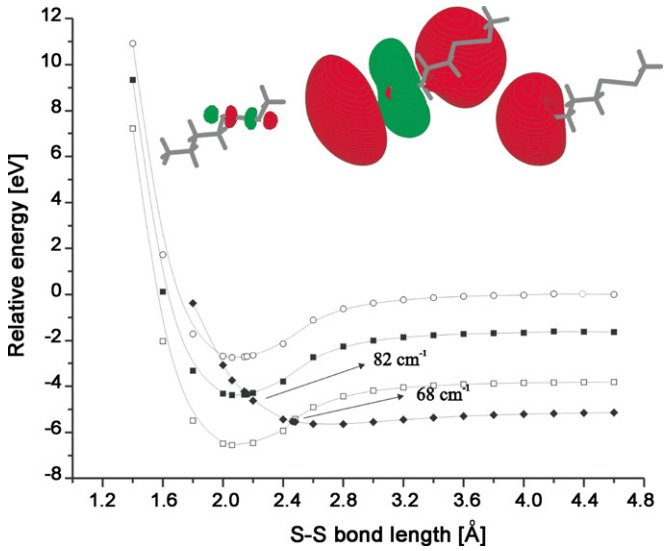

Fig. 4. Energies of the parent $H_3C—S—S—(CH_2)_3—NH_3^+$ cation (open circles), ground Rydberg-attached (open squares), excited Rydberg-attached (filled squares), and S—S σ*-attached (filed diamonds) states as functions of the S—S bond length.

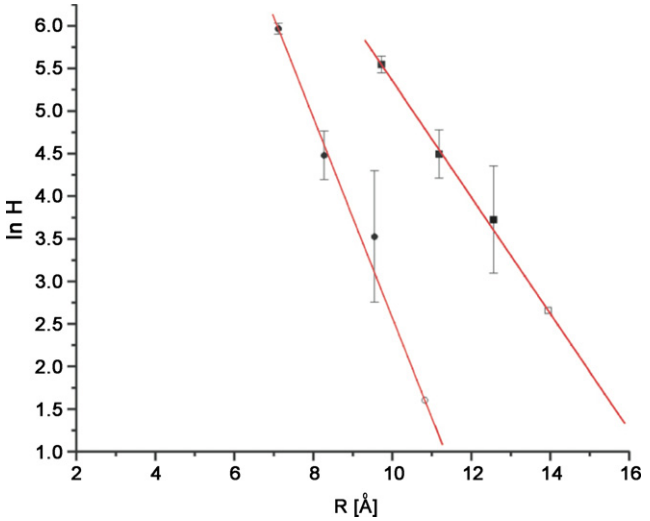

Fig. 6. Variation of the natural logarithm of the $H_{1,2}$ couplings between the S—S σ* and ground Rydberg (left curve) or S—S σ* and excited Rydberg (right curve) states as functions of the distance R between the pairs of orbitals.

cannot rule out the possibility that cleavage of the N—C_α bonds in the four Ala units closest to the Lys termini occurs by through-bond transfer from Lys, but most of our evidence aligns against this. First, there are more than 4–5 bonds separating the Lys' $—NH_3^+$ nitrogen atom and all but the closest of the Ala OCN units. Second, because the $H_{1,2}$ couplings decay exponentially with distance, one would expect the yield of N—C_α cleavage to also decay sharply as the distance to the Lys terminus increases; to our knowledge, the yields for cleaving all four of the Ala N—C_α bonds near the Lys termini do not differ considerably. For these reasons, we believe that the preponderance of experimental data and theoretical findings suggest that it is through Coulomb-stabilized direct electron attachment that the S—S and N—C_α cleavages occur for the compound shown in Fig. 3.

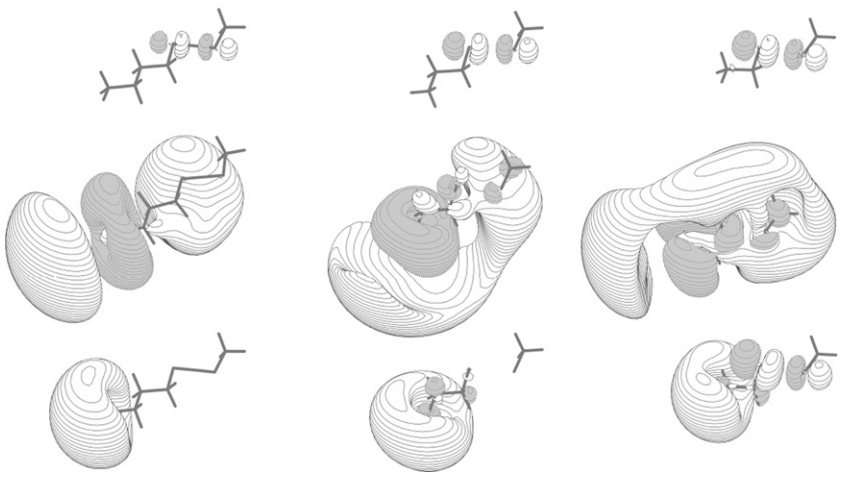

Fig. 5. S—S σ* (top), excited Rydberg (middle), and ground Rydberg (bottom) orbitals for n = 3 (left), 2 (center), and 1 (right) species. All orbitals have outermost contours within which 60% of the electron density is contained.

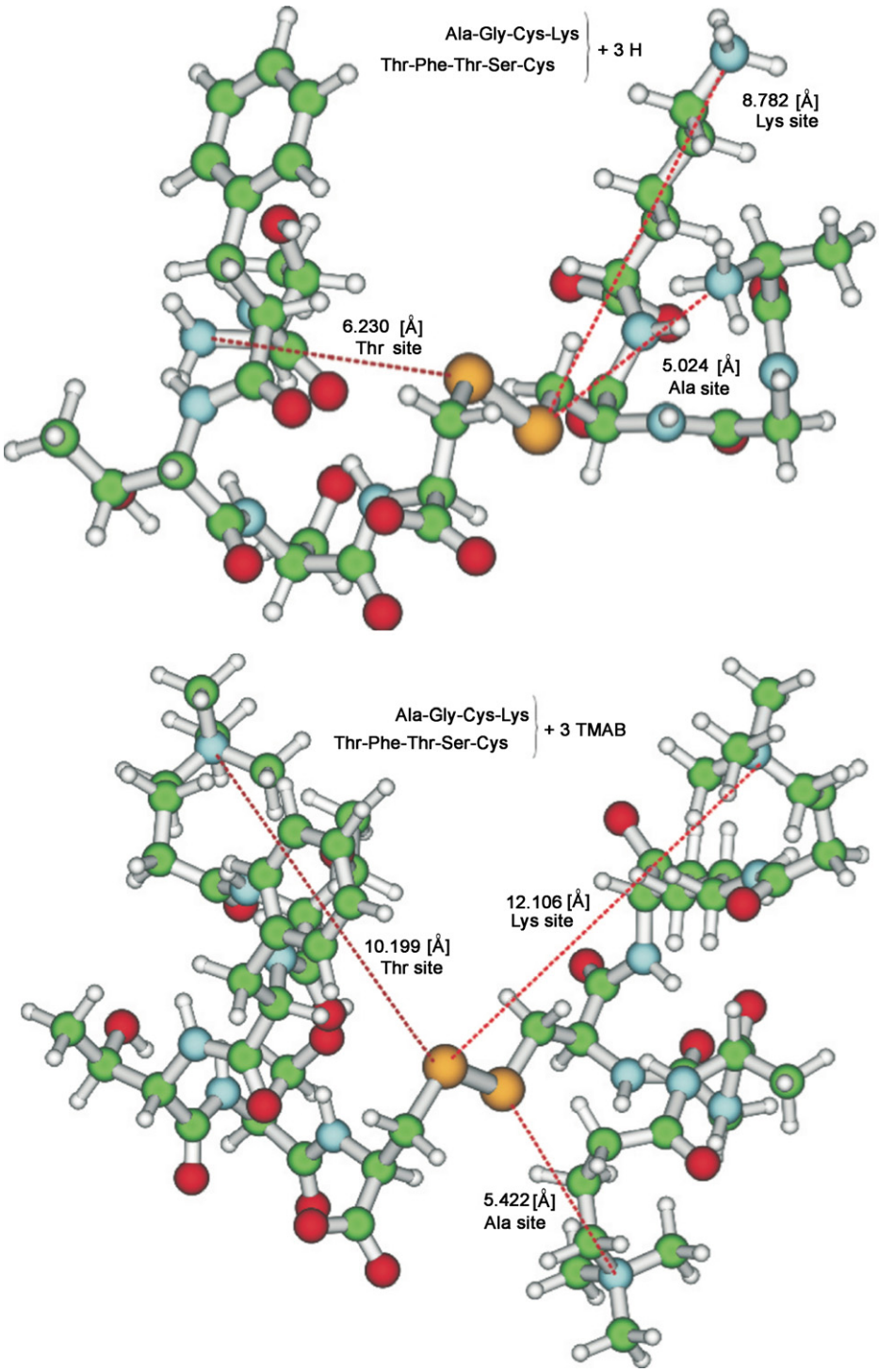

Fig. 7. Triply positively charged ions containing protonated side chains (top) or fixed-charge side chains (bottom) used in the experiments of Ref. [2e].

Our studies of through-space electron transfer were motivated by ETD data from the McLuckey lab [2e] in which S—S bond cleavage was observed to be a significant channel in the fragmentation of two kinds of ions shown in Fig. 7.

Based on the McLuckey data, we were faced with addressing two issues:

1. Could an electron initially attached to a Rydberg orbital of a protonated or fixed-charge side chain transfer (through space) to the S—S σ^* orbital when the Rydberg orbital comes into spatial overlap with the σ^* orbital?
2. Can an electron initially attached to a protonated or fixed-charge site migrate to another such site as the Rydberg orbitals on the two positive sites come into spatial overlap?

To address the first question, we computed and examined the energy profiles for model systems composed of a MeS–SMe molecule with either an NH_4^+ ion (to simulate a protonated site)

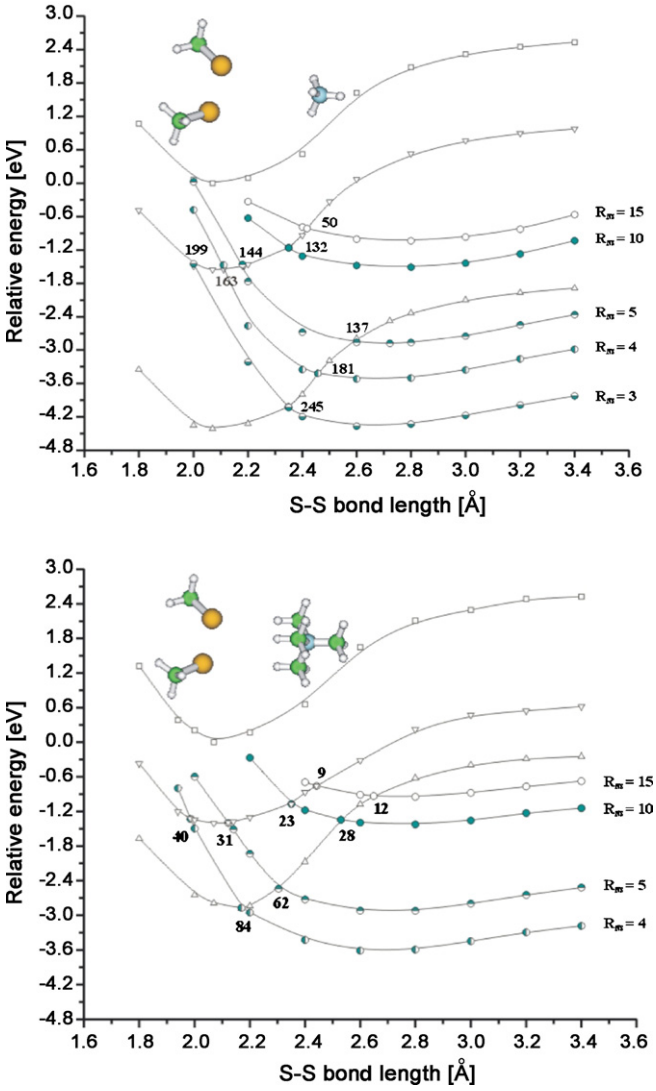

Fig. 8. Energies, as functions of the S—S bond length, of parent cation (open squares), ground Rydberg-attached (open triangles), excited Rydberg-attached (inverted open triangles), and S—S σ*-attached states (circles for various S—N distances R_{NS} in Å). The top figure corresponds to a protonated site, while the bottom figure relates to a fixed-charge site.

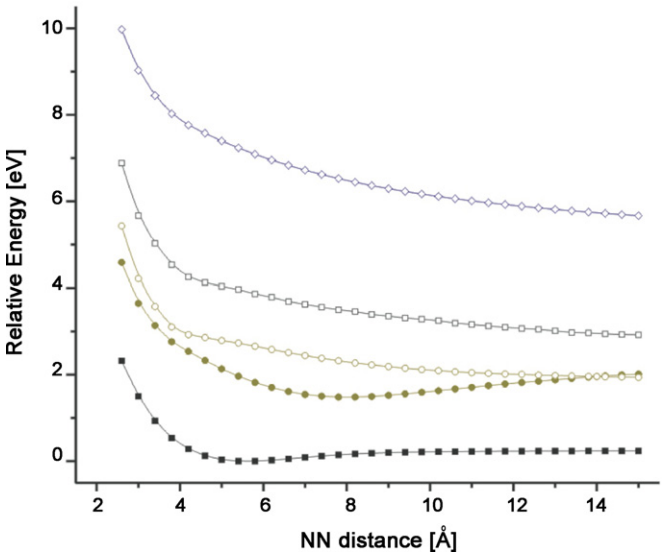

Fig. 9. Energies of low-lying electronic states of $[NH_4 \cdots N(CH_3)_4]^+$ as functions of the distance between the two nitrogen atoms. The energy of the system with no electron attached is shown in open diamonds.

or an $N(CH_3)_4^+$ ion (to simulate a fixed-charge site) at various distances R_{NS} from one another. In Fig. 8 we show the energy profiles, along the S—S bond axis, of the parent cation, the species with an electron attached to a ground or excited Rydberg orbital of the positive site, and the species with an electron attached to the S—S σ* orbital with the positive site at various distances R_{NS} away.

Also shown in Fig. 8 are the values of the $H_{1,2}$ couplings that pertain to electron migration from the Rydberg states to the S—S σ* states at each curve crossing. In Ref. [3p], we showed that these couplings also decay exponentially with the distance R_{NS} between the two sites over which electron transfer takes place.

By identifying the R_{NS} distances at which the S—S σ* state's curve crosses the ground or excited Rydberg curve near the equilibrium S—S bond length, we were able to say how close the protonated or fixed-charge site must come to the S—S bond to effect through-space electron transfer. As the data shown in Fig. 8 indicate, the positive site must come within ca. 5 Å of the S—S bond for electron transfer to occur. Moreover, because protonated and fixed-charge side chains are known to decay, by N—H or N—C bond cleavage, within a few μs after electron attachment, these findings suggest that the protonated or fixed-charge site must be within 5 Å of the S—S bond at the time ECD or ETD electron attachment takes place.

To address the second question posed above, we computed potential surfaces for several low-energy electronic states of a model system composed of an electron bound to a framework consisting of an NH_4^+ ion (to simulate a protonated site) and an $N(CH_3)_4^+$ ion (to simulate a fixed-charge site) separated by various distances. In Fig. 9, we show the energies of several such electronic states as functions of the distance between the two nitrogen atoms.

Because the ground and various excited Rydberg orbitals of protonated and fixed-charge sites have different energies (due to the differential shielding of the positive charge in the two species), the states shown in Fig. 9 correlate to either protonated or fixed-charge states at large N—N distances. For example, the state shown in filled squares corresponds to ground-Rydberg NH_4 plus an $N(CH_3)_4^+$ ion far away. The next two states correlate to excited NH_4 plus an $N(CH_3)_4^+$ ion, while the fourth state relates to NH_4^+ far away from $N(CH_3)_4$ in its ground-Rydberg state. The most important aspect of the data shown in Fig. 9 is that there are no crossings between states that correlate to NH_4 with those correlating to $N(CH_3)_4$. This finding allowed us to conclude that there is too much of an energy gap between the Rydberg states of protonated and fixed-charge (at least of the type modeled by $N(CH_3)_4^+$) sites to permit efficient through-space electron transfer via surface hopping.

Thus, with regard to the kind of species studied by McLuckey and illustrated in Fig. 7, we suggested that some of the S—S bond cleavage occurs by Coulomb-stabilized electron attachment to the S—S σ* orbital and that through-bond electron transfer was unlikely. Regarding the possibility of through-space transfer, we suggested that transfer between protonated and fixed-charge sites is probably not facile, although it may be for transfer from one protonated (or fixed-charge) site to another. The latter conclusions allowed us to offer (see p. 163 of Ref. [3p]) a rationalization of the McLuckey group's data in terms of a model in which

a. It is assumed that synthesis of the fixed-charge species shown in Fig. 7 containing zero, one, or two fixed-charge sites (the

remainder being protonated sites) retains the Ala site in protonated form (in Ref. [3p] it is argued that this lowers the internal Coulomb repulsion and thus the thermodynamic stability of the ion).

b. For species containing zero or three fixed-charge sites, electron attachment to a charged site can, via through-space transfer, allow the attached electron to migrate to the Ala site, which is closest to the S—S bond, and thus to subsequently transfer from the Ala site to the S—S σ^* orbital. It was suggested this is why compounds containing zero or three fixed-charge sites have the highest yield of S—S bond cleavage.
c. For species containing two fixed-charge sites (by assumption on the Thr and Lys side chains) any electrons captured at the (fixed-charge modified) Thr or Lys sites cannot be transferred to the nearby Ala site, so S—S bond cleavage is low for such species. Only electrons that attach to the (protonated) Ala site or that attach directly to the S—S σ^* orbital can cleave the S—S bond.
d. Species with one fixed-charge site should have intermediate yields of S—S bond cleavage because they can fragment by direct attachment to the S—S σ^* orbital, by attachment to the nearby (protonated) Ala site, or by attachment to whichever of the Thr or Lys sites is protonated followed by through-space transfer to the Ala site and subsequent transfer to the S—S σ^* orbital.

These trends in S—S bond cleavage yields are what was seen in Ref. [2e].

3. Strategy in the present work and methods used

In the present work, we extend the kind of studies outlined above in two directions:

1. We consider the possibility that through-bond electron transfer can be more facile if the spacer groups separating the S—S bond and the positive site involve olefinic as well as aliphatic linkages. In our earlier work, we used $-(CH_2)_n-$ units to connect the two sites; in the present work, we employ a $-CH{=}CH-(CH_2)_n-$ spacer.
2. We examine the possibility of through-space electron transfer between fixed-charge sites of different electron binding strengths. In our earlier work, we considered transfer from a protonated amine site to an $N(CH_3)_4^+$ site. Now, we will consider electron transfer between an $N(CH_3)_4^+$ and a $C(NH_2)_3^+$ ion representative of the positive site in protonated arginine. These two sites have Rydberg orbitals with considerably closer electron binding energies than do NH_4^+ and $N(CH_3)_4^+$.

Based on our earlier experience in electron transfer modeling, we decided to first perform our calculations at the Hartree–Fock (HF) self-consistent field (SCF) level of theory and to then extend our investigations to the unrestricted second-order Møller–Plesset (UMP2) level of theory.

In our studies of through-bond electron transfer in $H_3C-S-S-CH{=}CH-(CH_2)_n-NH_3^+$, the structures (bond lengths and angles) were first partially optimized at the Hartree–Fock level with the distance between the nitrogen atom and the midpoint of the sulfur–sulfur bond held fixed throughout the optimization calculations. Then in subsequent UMP2 calculations, we retained this frozen geometry because we were attempting to model the environment within a peptide or protein in which an S—S σ^* orbital is Coulomb stabilized by a positively charged site whose location remains quite fixed. In addition, we wanted to extract information about the distance-dependence of the electron transfer rates, so it was important to have the distance from the S—S bond to the $-NH_3^+$ site held fixed. In our studies of through-space electron transfer between $N(CH_3)_4^+$ and $C(NH_2)_3^+$, we froze the distance between the nitrogen and carbon atoms of the respective cations while optimizing other internal coordinates.

The addition of one set (1s1p) of extra-diffuse basis functions [6] centered on the positive sites' central atom to the aug-cc-pVDZ basis sets [7] was necessary to properly describe the ground and excited Rydberg states of the NH_4, $N(CH_3)_4$ and $C(NH_2)_3$ species. This kind of basis was shown earlier [6] to be capable of reproducing the energies of such low-energy Rydberg states of nitrogen-centered radicals. With only four such extra diffuse functions in our basis, the number of Rydberg levels that we can describe is, of course, limited.

To evaluate the probabilities for electron transfer in our through-bond study, we generated the necessary energy surfaces at the unrestricted second-order Møller–Plesset (UMP2) level and examined the energies of the ground-Rydberg, excited-Rydberg, and S—S σ^*-attached states as functions of the S—S bond length (with the other internal coordinates of $H_3C-S-S-CH{=}CH-(CH_2)_n-NH_3^+$ held fixed for the reasons noted earlier). The use of an unrestricted method was necessary both to achieve a qualitatively correct description of the homolytic cleavage of the S—S bond and because the various electron-attached species are open-shell systems. Because the methods we used are based on an unrestricted Hartree–Fock starting point, it is important then to make sure that little, if any, artificial spin contamination enters into the final wave functions. We computed $\langle S^2 \rangle$ for species studied in this work and found values not exceeding (after annihilation) the expected value of 0.75 by more than 0.06 in all open-shell doublet neutral cases.

Special difficulties arise when carrying out computations of not just the lowest-energy electron-attached state at each S—S bond length, but the energies of several such states. In such cases, great care must be taken to avoid variational collapse. For the ground-Rydberg state, this was not an issue, but it was for the excited-Rydberg state and for the σ^*-attached state at some geometries. For the excited-Rydberg case, we found it adequate to use the "alter" option in the Gaussian program to begin the iterative SCF process with the desired orbital occupancy. Convergence to the desired (excited Rydberg) state was then verified by visually inspecting the singly occupied orbital after convergence. For the state in which the electron is attached to the S—S σ^* orbital, we had to use another approach because variational collapse took place during the SCF iterations even when we used the "alter" option. In the method we used to overcome the problem for this state, we introduced a device that we have employed in many past applications [8]. Specifically, we artificially increased the nuclear charges by a small amount δq of the atoms (the sulfur atoms for the S—S σ^* state) involved in accepting the transferred electron, and carried out the UMP2 calculations with these artificial nuclear charges. By plotting the energies of the states for several values of the charge increment δq and extrapolating to $\delta q = 0$, we were able to evaluate the true energy of these states.

In our study of through-space electron transfer between $N(CH_3)_4$ and $C(NH_2)_3$, we had to evaluate the energies of the ground- and several excited-Rydberg states. To avoid the misery of variational collapse in this case, we employed the outer valence Greens function (OVGF [9]) option within the Gaussian code. In this way, we obtained the energies of the various electron-attached states in terms of OVGF electron attachment energies of the parent $[N(CH_3)_4 \cdots C(NH_2)_3]^{2+}$ doubly charged species.

Finally, we note that all calculations were performed using the Gaussian 03 suite of programs [10], and the three-dimensional plots of the molecular orbitals were generated with the MOLDEN program [11].

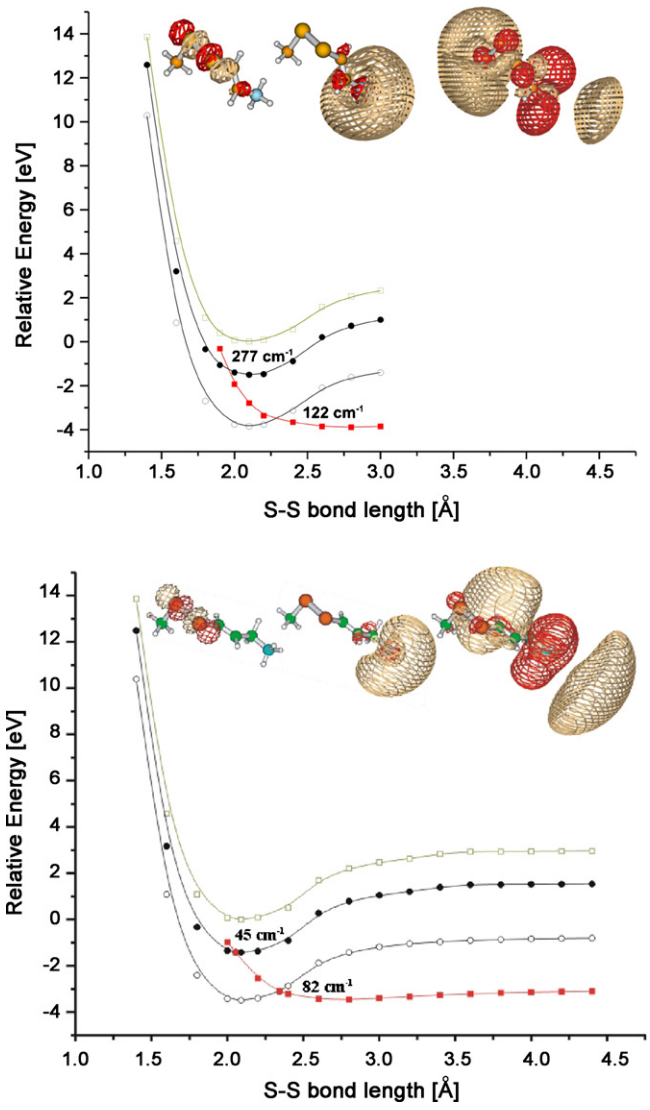

Fig. 10. MP2-level energies of the parent $H_3C{-}S{-}S{-}CH{=}CH{-}(CH_2)_n{-}NH_3^+$ cations (open squares) and of the species in which an electron is attached to the ground-Rydberg orbital (open circles), the excited-Rydberg orbital (filled circles), and the S—S σ* orbital (filled squares) as functions of the S—S bond length. The top figure is for $n = 0$ and the bottom is for $n = 1$. The MP2-level $H_{1,2}$ coupling matrix elements are also shown as are the S—S σ*, ground and excited-state Rydberg orbitals from left to right.

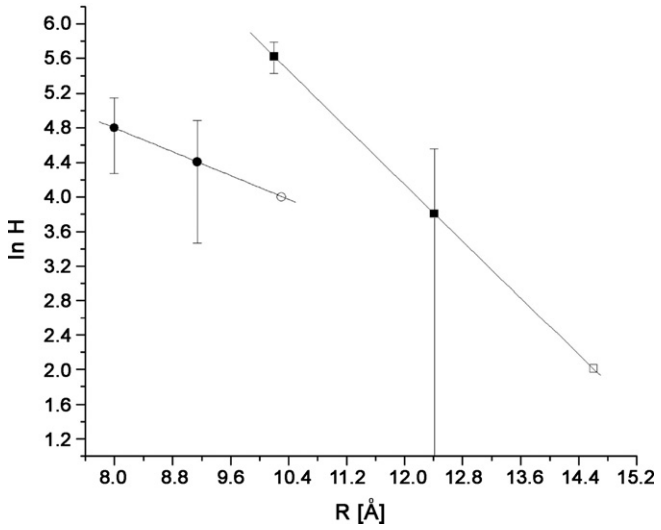

Fig. 11. Variation of the $H_{1,2}$ coupling matrix elements as functions of the distance R between the mid-point of the S—S bond and the centroid of the Rydberg orbital (ground or excited) for the ground (left) and excited (right) Rydberg state coupling to the S—S σ* state. The error bars indicate 50 cm^{-1} uncertainty in the values of the $H_{1,2}$ elements. The open square symbols show the value of $\ln H_{1,2}$ obtained by extrapolation to a compound containing 2 methylene units and one olefinic unit.

4. Results

4.1. Through-bond electron transfer

In Fig. 10, we show the energy profiles pertinent to electron attachment to two of our model compounds $H_3C{-}S{-}S{-}CH{=}CH{-}(CH_2)_n{-}NH_3^+$ as functions of the S—S bond length. Also shown are the S—S σ*, ground, and excited Rydberg orbitals and the $H_{1,2}$ couplings associated with each curve crossing.

In Fig. 11, we plot the natural logarithm of the $H_{1,2}$ couplings as functions of the distance between the S—S bond and the outermost point on the ground- or excited-Rydberg orbital contour within which 60% of the electron density is contained (we call this the centroid). We made this choice for defining the distance between the orbitals to be consistent with what we plotted in Ref. [3q] where we studied through-bond transfer for species of the type $H_3C{-}S{-}S{-}(CH_2)_n{-}NH_3$.

One conclusion from the present work can be reached by comparing the magnitudes of the $H_{1,2}$ elements that arise in the present $H_3C{-}S{-}S{-}CH{=}CH{-}(CH_2)_n{-}NH_3^+$ model compounds to those found for the compounds $H_3C{-}S{-}S{-}(CH_2)_n{-}NH_3^+$ containing only aliphatic linkages in the spacer groups. As one can glean from Figs. 6 and 11, the distances between the S—S bond and the centroids of the ground and excited Rydberg orbitals in $H_3C{-}S{-}S{-}(CH_2)_2{-}NH_3^+$ are very close to those in $H_3C{-}S{-}S{-}CH{=}CH{-}NH_3^+$, and the distances in $H_3C{-}S{-}S{-}(CH_2)_3{-}NH_3^+$ are close to those in $H_3C{-}S{-}S{-}CH{=}CH{-}(CH_2){-}NH_3^+$. These similarities in distances are, of course, not surprising because an olefinic linkage —C=C— is similar in length to two methylene units (Table 1).

From these data, we conclude that through-bond electron transfer over 3–5 bonds spanning a given distance is not qualitatively different if all of these bonds involve aliphatic linkages or one of the bonds is olefinic. That is, we do not see any reason to expect a major enhancement in through-bond transfer when olefinic link-

Table 1
Coupling strengths (cm^{-1}) between ground or excited Rydberg states and S—S σ* state for aliphatic (data on the left) and mixed olefinic/aliphatic (data on the right) spacers

Species	$H_{1,2}^{grnd}$	$H_{1,2}^{ex}$	$H_{1,2}^{grnd}$	$H_{1,2}^{ex}$	Species
$H_3C{-}S{-}S{-}(CH_2){-}NH_3^+$	781[a]	809[a]			
$H_3C{-}S{-}S{-}(CH_2)_2{-}NH_3^+$	353[a]	354[a]	122	277	$H_3C{-}S{-}S{-}CH{=}CH{-}NH_3^+$
$H_3C{-}S{-}S{-}(CH_2)_3{-}NH_3^+$	68[a]	82[a]	82	45	$H_3C{-}S{-}S{-}CH{=}CH{-}(CH_2){-}NH_3^+$
$H_3C{-}S{-}S{-}(CH_2)_4{-}NH_3^+$	5[b]	15[b]	49[b]	7[b]	$H_3C{-}S{-}S{-}CH{=}CH{-}(CH_2)_2{-}NH_3^+$

[a] These data first appeared in Ref. [3q].
[b] Values for these longer compounds were obtained from extrapolating as indicated in Figs. 6 and 11.

ages are present. Therefore, the conclusions we reached earlier in Ref. [3q] should remain valid even when the bonds connecting the Rydberg and S—S σ^* orbitals are not all aliphatic.

It was shown in Ref. [3q] that coupling strengths in the 300 cm^{-1} range produce surface-hopping probabilities (using Landau-Zener theory) of ca. 0.1–0.5 [12]. Thus, as long as the S—S σ^* curve intersects the ground or excited Rydberg curve near the equilibrium S—S bond length (so the crossing is accessible by thermal motions of this bond), we can estimate the rates of through-bond electron transfer by multiplying the S—S vibrational frequency ν_{SS} (ca. 1.5×10^{13} s^{-1}) by the surface hopping probability (0.1–0.5) and then scaling by the ratio of the square of $(H_{1,2}/300)$:

$$\text{Rate} \approx (1.5\text{–}7.5) \times 10^{12} \left(\frac{H_{1,2}}{300}\right)^2 \text{s}^{-1}. \quad (1)$$

For the through-bond migration to be effective in cleaving the S—S bond, it must occur before the Rydberg species from which the electron is transferred can decay by some other mechanism. It is believed that electron attachment (in ECD or ETD) at a positively charged side chain initially occurs into an excited Rydberg orbital after which a decay cascade leads to formation of the ground Rydberg species. It is known [13] that excited Rydberg states belonging to protonated or fixed-charge amine site undergo radiationless relaxation to the ground Rydberg state in a few μs. Moreover, we know that the excited Rydberg states do not decay by N—H or N—C bond cleavage, but the ground Rydberg states do (in ca. 10^{-12} s). Hence, to be effective in cleaving an S—S bond, the through-bond electron transfer must occur within ca. 10^{-6} s of the time the electron attaches to an excited Rydberg orbital. This fact allows us to estimate the smallest $H_{1,2}$ coupling strength that could produce S—S bond cleavage by solving Eq. (1) for a rate of ca. 10^6 s^{-1}. This gives an estimate of $H_{1,2}^{\min} = 0.11\text{–}0.24$ cm^{-1}. Using the data shown in Figs. 6 and 11 with this range of $H_{1,2}^{\min}$ values, we conclude that through-bond electron transfer can occur at a rate capable of yielding S—S bond cleavage if there are up to 7 bonds (aliphatic or olefinic) separating the sulfur and nitrogen atoms.

4.2. Through-space electron transfer from one positive site to another

In our earlier study [3p] of through-space electron transfer between positive sites, we used NH_4^+ and $N(CH_3)_4^+$ to represent protonated amine and fixed-charge sites. As shown earlier in the discussion surrounding Fig. 9, that study allowed us to conclude that the electron binding strengths for the Rydberg orbitals of NH_4^+ and $N(CH_3)_4^+$ (4.5 eV and 2.5 eV, respectively, for the ground-state Rydberg orbitals) differ so much that curve crossings do not occur (at least for lower states), as a result of which electron transfer between such sites is unlikely. In Fig. 12, we show the ground and (first) excited Rydberg orbitals associated with the two positive sites considered in the present study. These orbitals are shown at a separation between the two sites corresponding to the minimum-energy for the ground state of $[N(CH_3)_4\cdots C(NH_2)_3]^+$. At such distances, one can see that the Rydberg orbitals of the two sites overlap considerably. One of the positive species $N(CH_3)_4^+$ is chosen to simulate a fixed-charge side chain's positive site, while the other $C(NH_2)_3^+$ is chosen to simulate protonated arginine's positive site. These two species have ground-state electron binding energies that differ by ca. 0.5 eV (in contrast to the >2 eV energy difference for NH_4^+ and $N(CH_3)_4^+$), so we expect that electron transfer between them may be possible.

In Fig. 13, we show the energy profiles, as functions of the inter-ion distance, of the ground and several low-energy states of the $N(CH_3)_4^+\cdots C(NH_2)_3^+$ system to which one electron is attached.

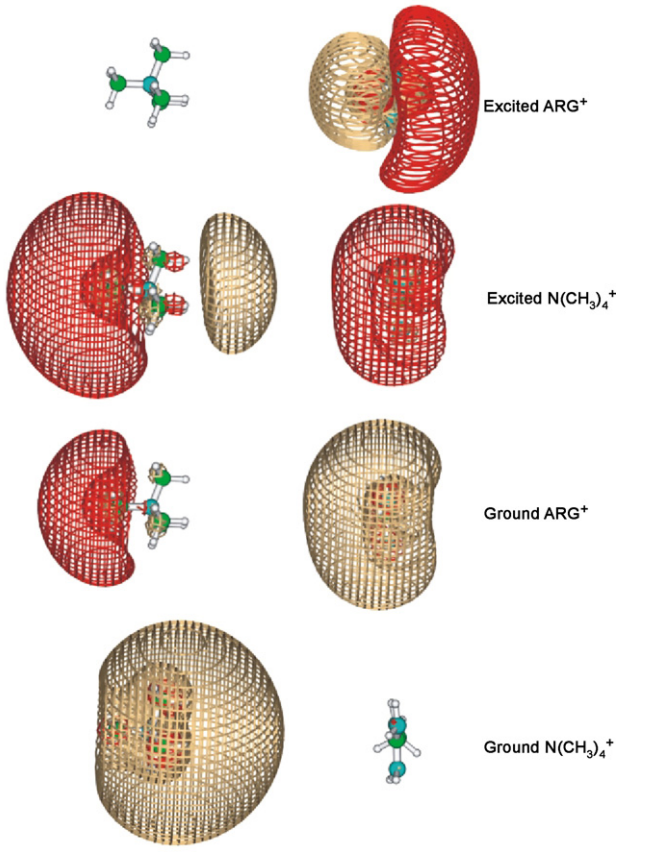

Fig. 12. Ground and low-energy excited Rydberg orbitals of the $N(CH_3)_4^+\cdots C(NH_2)_3^+$ species evaluated at the inter-ion distance corresponding to the minimum on the energy surface of the lowest state of $[N(CH_3)_4\cdots C(NH_2)_3]^+$. The four orbitals shown correlate, at large inter-ion separation, to the ground and lowest Rydberg states of $N(CH_3)_4^+$ and of $C(NH_2)_3^+$ as labeled.

The nature of some of the states (i.e., whether they are dominantly arginine or $N(CH_3)_4^+$ localized) was difficult to determine (i.e., they were very "mixed"). In these cases, we have not labeled them in Fig. 13.

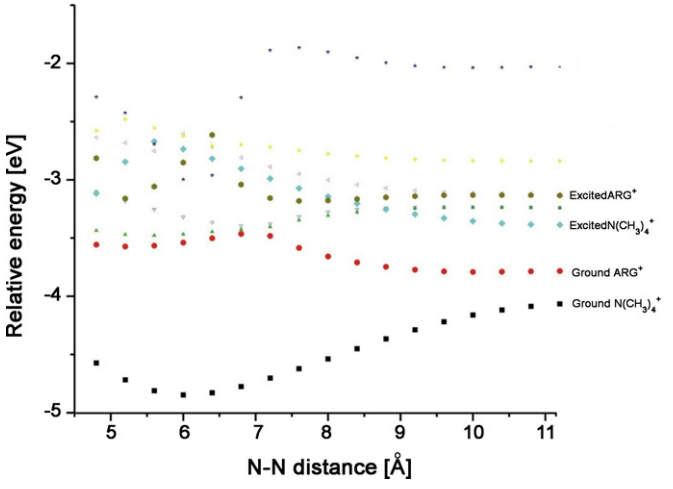

Fig. 13. Energies of the ground and low-lying excited states of $[N(CH_3)_4\cdots C(NH_2)_3]^+$ with the species and state to which these states correlate at large inter-ion distance labeled on the right.

Nevertheless, the data of Fig. 13 suggest that, aside from the lowest-energy state, there are numerous curve crossings that, in turn, tell us that

a. An electron initially bound to the ground Rydberg state of $N(CH_3)_4^+$ will not transfer to $C(NH_2)_3^+$ because the ground-state curve (filled squares), which correlates to ground-state $N(CH_3)_4$ plus $C(NH_2)_3^+$, does not undergo a crossing with any other state. Most likely, such a $N(CH_3)_4$ species (i.e., the side chain it represents) will undergo N—CH_3 bond cleavage as discussed earlier in this paper.
b. An electron initially bound to the ground Rydberg state of $C(NH_2)_3^+$ can transfer to an excited Rydberg state of $N(CH_3)_4^+$ because the surface (filled circles) correlating to ground-state $C(NH_2)_3$ undergoes crossings with states that correlate to excited Rydberg states of $N(CH_3)_4^+$.
c. An electron initially bound to an excited Rydberg state of $N(CH_3)_4^+$ can transfer to a Rydberg state (excited or ground) of $C(NH_2)_3^+$ because the curves associated with such excited states undergo crossings that permit these events.
d. An electron initially bound to an excited Rydberg state of $C(NH_2)_3^+$ can transfer to a Rydberg state (excited or ground) of $N(CH_3)_4^+$ because the curves associated with such excited states undergo crossings that permit these events.

So, the combination of our earlier studies (using NH_4^+ and $N(CH_3)_4^+$) and the present findings (using $N(CH_3)_4^+$ and $C(NH_2)_3^+$) suggest that through-space electron transfer from one positively charged side chain to another can occur but

a. not from the ground Rydberg state of the side chain having the highest electron binding strength, and
b. only if the electron binding strengths of the two side chains are similar (e.g., as in $N(CH_3)_4^+$ and $C(NH_2)_3^+$ where they differ by ca. 0.5 eV).

Of course, the excited Rydberg states of all these species can also undergo radiationless relaxation to lower states in μs timescales. Moreover, the ground Rydberg states may be susceptible to decay by bond cleavage (over timescales of ca. 10^{-12} s).

As Fig. 13 suggests, there are multiple curve crossings among the excited Rydberg states belonging to the two charged sites. Although we were able, in our earlier study of through-bond electron transfer in which few such crossings appear, to extract $H_{1,2}$ couplings, we do not feel confident in doing so in the present through-space transfer study. There are just too many crossings and they are not even "isolated" in the sense that only two curves are in close proximity near a given crossing. For this reason, we do not venture to approximate the rates (i.e., use Landau-Zener theory) for the through-space transfer processes studied here. We prefer to simply use the data from Fig. 13 to conclude that through-space electron transfer can occur for species with electron binding energies differing by ca. 0.5 eV as in our model systems.

5. Summary

The primary findings of the present study are

1. That through-bond electron transfer rates through combined olefinic-and-aliphatic linkages are not qualitatively different than through aliphatic linkages of similar length.
2. That through-bond transfer can occur from Rydberg orbitals of protonated or fixed-charge sites to S—S bonds at experimentally relevant rates but only over ca. 7 intervening bonds.
3. That through-space transfer from a Rydberg orbital of one positive side chain to a Rydberg orbital of another side chain can occur but only if the electron binding strengths of the two side chains' Rydberg orbitals are similar.

When applied to the data [5] obtained in the Marshall group on the species shown in Fig. 3, these findings suggest that it is highly unlikely that the disulfide cleavage, which was found to occur in substantial amounts, could arise from initial electron attachment at one of the charged Lys termini followed by through-bond electron transfer to the S—S bond. There are just too many intervening bonds. Moreover, the rigidity of the $(Ala)_n$ helices do not allow the charged Lys to come close enough to the S—S bond to allow through-space transfer from Lys to the S—S bond. Therefore, we are left concluding that the disulfide cleavage in these species most likely arises from direct Coulomb-assisted electron attachment to the S—S σ* orbital as first suggested in Ref. [3j].

In the Marshall-group data [5], some cleavage of N—C_α bonds occurred within the four Ala units closest to the charged Lys termini. Our present findings cannot rule out that these cleavages take place by through-bond electron transfer from a Lys terminus to an Ala OCN π* orbital. However, if this were the dominant mechanism, one would expect to see an exponential decrease in the yield of N—C_α cleavage as the distance from the cleaved Ala to the Lys increases. The data of Ref. [5] do not seem to show such a decrease along the Ala chain, so this argues against through-bond electron transfer being the dominant mechanism. What about through-space electron transfer from a Rydberg orbital of Lys to the nearby Ala OCN π* orbitals? We are not convinced that the length and flexibility of the Lys side chain are adequate to allow the Lys terminus to come close enough to the fourth Ala from the Lys terminus, but, until we (or someone else) carry out molecular dynamics simulations, we cannot further exclude this possibility. However, geometric arguments alone argue that the frequency with which a Lys —NH_3 unit encounters, via thermal motions, an Ala OCN π* orbital would vary

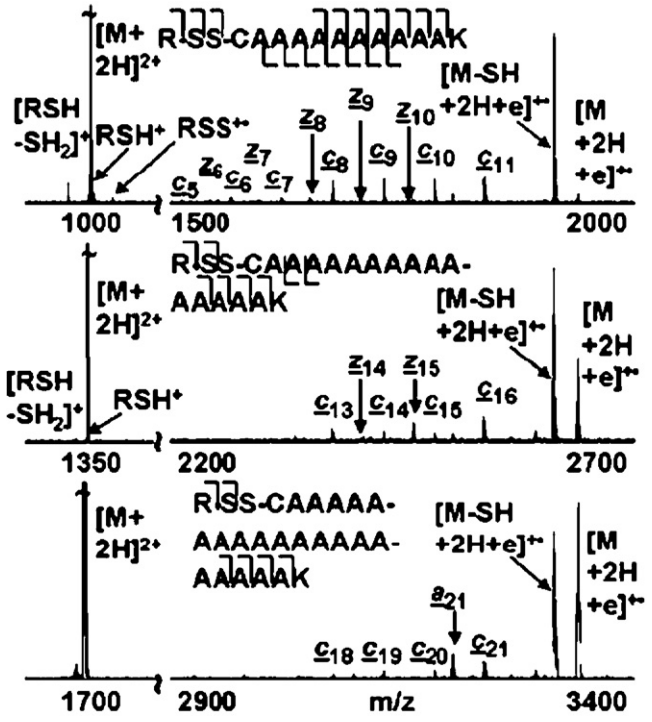

Fig. 14. Fragmentation patterns found by the Marshall group [5] for species $(AcCA_nK+H)_2^{2+}$ shown in Fig. 3 (taken from ref. [5]).

inversely as the square of the distance between the Lys and Ala orbitals. This, in turn, suggests that the yield of N—C_α cleavage within the four Ala units closest to the Lys termini should vary in like fashion. However, the fragmentation patterns of Ref. [5], which we reproduce in Fig. 14, show very similar yields for cleaving the four Ala N—C_α units closest to the Lys termini.

For example, for $(AcCA_{15}K+H)_2^{2+}$, we see in Fig. 14, fragment ions c_{16}, c_{15}, c_{14}, and c_{13} in similar abundances. It is for these reasons that we think the N—C_α cleavage of the four Ala units closest to the Lys termini also most likely occurs by direct Coulomb-assisted electron attachment to the corresponding OCN π orbitals. However, we admit that sufficient data to be confident in this claim are still lacking.

The observations of the present work also relate to findings from the McLuckey lab [2e] on species similar to those shown in Fig. 7. In particular, our data suggest that electron transfer among positively charged sites on side chains can take place but only if the electron binding energies of the Rydberg orbitals on these sites are similar (e.g., differing by ca. 0.5 eV but not by 2 eV or more). Small differences in binding energies allow the attractive interactions between two charged side chains (once an electron is attached to one) to induce curve crossings and thus to effect electron transfer.

Acknowledgements

This work has been supported by NSF Grant No. 0240387 to J. S. Significant computer time provided by the Center for High Performance Computing at the University of Utah is also gratefully acknowledged.

References

[1] (a) R.A. Zubarev, N.L. Kelleher, F.W. McLafferty, J. Am. Chem. Soc. 120 (1998) 3265;
(b) R.A. Zubarev, N.A. Kruger, E.K. Fridriksson, M.A. Lewis, D.M. Horn, B.K. Carpenter, F.W. McLafferty, J. Am. Chem. Soc. 121 (1999) 2857;
(c) R.A. Zubarev, D.M. Horn, E.K. Fridriksson, N.L. Kelleher, N.A. Kruger, M.A. Lewis, B.K. Carpenter, F.W. McLafferty, Anal. Chem. 72 (2000) 563;
(d) R.A. Zubarev, K.F. Haselmann, B. Budnik, F. Kjeldsen, F. Jensen, Eur. J. Mass Spectrom. 8 (2002) 337.

[2] (a) J.E.P. Syka, J.J. Coon, M.J. Schroeder, J. Shabanowitz, D.F. Hunt, Proc. Natl. Acad. Sci. 101 (2004) 9528;
(b) J.J. Coon, J.E.P. Syka, J.C. Schwartz, J. Shabanowitz, D.F. Hunt, Int. J. Mass Spectrom. 236 (2004) 33;
(c) S.J. Pitteri, P.A. Chrisman, S.A. McLuckey, Anal. Chem. 77 (2005) 5662;
(d) H.P. Gunawardena, M. He, P.A. Chrisman, S.J. Pitteri, J.M. Hogan, B.D.M. Hodges, S.A. McLuckey, J. Am. Chem. Soc. 127 (2005) 12627;
(e) H.P. Gunawardena, L. Gorenstein, D.E. Erickson, Y. Xia, S.A. McLuckey, Int. J. Mass Spectrom. 265 (2007) 130.

[3] (a) E.A. Syrstad, F. Turecek, J. Phys. Chem. A105 (2001) 11144;
(b) F. Turecek, E.A. Syrstad, J. Am. Chem. Soc. 125 (2003) 3353;
(c) F. Turecek, M. Polasek, A. Frank, M. Sadilek, J. Am. Chem. Soc. 122 (2000) 2361 ;
(d) E.A. Syrstad, D.D. Stephens, F. Turecek, J. Phys. Chem. A107 (2003) 115;
(e) F. Turecek, J. Am. Chem. Soc. 125 (2003) 5954;
(f) E.A. Syrstad, F. Turecek, Am. Soc. Mass Spectrom. 16 (2005) 208;
(g) E. Uggerud, Int. J. Mass Spectrom. 234 (2004) 45;
(h) I. Anusiewicz, J. Berdys-Kochanska, J. Simons, J. Phys. Chem. A109 (2005) 5801;
(i) I. Anusiewicz, J. Berdys-Kochanska, P. Skurski, J. Simons, J. Phys. Chem. A110 (2006) 1261;
(j) A. Sawicka, P. Skurski, R.R. Hudgins, J. Simons, J. Phys. Chem. B107 (2003) 13505;
(k) M. Sobczyk, P. Skurski, J. Simons, Adv. Quantum Chem. 48 (2005) 239;
(l) A. Sawicka, J. Berdys-Kochaska, P. Skurski, J. Simons, Int. J. Quantum Chem. 102 (2005) 838;
(m) I. Anusiewicz, J. Berdys, M. Sobczyk, A. Sawicka, P. Skurski, J. Simons, J. Phys. Chem. A109 (2005) 250;
(n) V. Bakken, T. Helgaker, E. Uggerud, Eur. J. Mass Spectrom. 10 (2004) 625;
(o) P. Skurski, M. Sobczyk, J. Jakowski, J. Simons, Int. J. Mass Spectrom. 265 (2007) 197;
(p) M. Sobczyk, D. Neff, J. Simons, Int. J. Mass Spectrom. 269 (2008) 149;
(q) M. Sobczyk, J. Simons, Int. J. Mass Spectrom. 253 (2006) 274;
(r) M. Sobczyk, J. Simons, J. Phys. Chem. B 110 (2006) 7519.

[4] C. Dezarnaud-Dandine, F. Bournel, M. Troncy, D. Jones, A. Modelli, J. Phys. B: At. Mol. Opt. Phys. 31 (1998) L497;
M. Seydou, A. Modelli, B. Lucas, K. Konate, C. Desfrancois, J.P. Schermann, Eur. Phys. J. D 35 (2005) 199.

[5] R. Hudgins, K. Håkansson, J.P. Quinn, C.L. Hendrickson, A.G. Marshall, Proceedings of the 50th ASMS Conference on Mass Spectrometry and Allied Topics, Orlando, Florida, June 2–6, 2002, A020420. Fig. 1 first appears in publication in Ref. [3j].

[6] (a) M. Gutowski, J. Simons, J. Chem. Phys. 93 (1990) 3874;
(b) P. Skurski, M. Gutowski, J. Simons, Int. J. Quantum Chem. 80 (2000) 1024.

[7] R.A. Kendall, T.H. Dunning Jr., R.J. Harrison, J. Chem. Phys. 96 (1992) 6796.

[8] See Ref. [3m]. This device was first used in B. Nestmann and S. D. Peyerimhoff, J. Phys. B 18 (1985) 615 and J. Phys. B 18 (1985) 4309.

[9] J.V. Ortiz, J. Chem. Phys. 89 (1988) 6348;
L.S. Cederbaum, J. Phys. B 8 (1975) 290;
W. von Niessen, J. Schirmer, L.S. Cederbaum, Comp. Phys. Rep. 1 (1984) 57;
V.G. Zakrzewski, W. von Niessen, J. Comp. Chem. 14 (1993) 13;
V.G. Zakrzewski, J.V. Ortiz, Int. J. Quantum Chem. 53 (1995) 583;
J.V. Ortiz, Int. J. Quantum Chem. Symp. 22 (1988) 431;
J.V. Ortiz, Int. J. Quantum Chem. Symp. 23 (1989) 321.

[10] M.J. Frisch, G.W. Trucks, H.B. Schlegel, G.E. Scuseria, M.A. Robb, J.R. Cheeseman, J.A. Montgomery Jr., T. Vreven, K.N. Kudin, J.C. Burant, J.M. Millam, S.S. Iyengar, J. Tomasi, V. Barone, B. Mennucci, M. Cossi, G. Scalmani, N. Rega, G.A. Petersson, H. Nakatsuji, M. Hada, M. Ehara, K. Toyota, R. Fukuda, J. Hasegawa, M. Ishida, T. Nakajima, Y. Honda, O. Kitao, H. Nakai, M. Klene, X. Li, J.E. Knox, H.P. Hratchian, J.B. Cross, C. Adamo, J. Jaramillo, R. Gomperts, R.E. Stratmann, O. Yazyev, A.J. Austin, R. Cammi, C. Pomelli, J.W. Ochterski, P.Y. Ayala, K. Morokuma, G.A. Voth, P. Salvador, J.J. Dannenberg, V.G. Zakrzewski, S. Dapprich, A.D. Daniels, M.C. Strain, O. Farkas, D.K. Malick, A.D. Rabuck, K. Raghavachari, J.B. Foresman, J.V. Ortiz, Q. Cui, A.G. Baboul, S. Clifford, J. Cioslowski, B.B. Stefanov, G. Liu, A. Liashenko, P. Piskorz, I. Komaromi, R.L. Martin, D.J. Fox, T. Keith, M.A. Al-Laham, C.Y. Peng, A. Nanayakkara, M. Challacombe, P.M.W. Gill, B. Johnson, W. Chen, M.W. Wong, C. Gonzalez, J.A. Pople, Gaussian, Inc., Wallingford, CT, 2004.

[11] G. Schaftenaar, J.H. Noordik, J. Comput. Aided Mol. Des. 14 (2000) 123.

[12] These probabilities also depend on the difference in slopes of the two surfaces at the point of crossing as well as the speed with which the S—S bond is moving at the crossing. However, all of the crossings studied in the present work and in ref. [3q] have similar values of these parameters. Hence, the surface hopping probability ratios can be estimated by comparing values of $(H_{1,2})^2$ which also enters into the Landau-Zener formula.

[13] F. Turecek, P.J. Reid, Int. J. Mass Spectrom. 222 (2003) 49.